Electronic Supplementary Material (ESI) for Journal of Materials Chemistry
This journal is © The Royal Society of Chemistry 2012

Electronic Supplementary Information

Hierarchical Optical Antenna: Gold Nanoparticles Modified Photonic Crystal for High-Sensitive Label-Free DNA Detection

Weizhi Shen, [†] Mingzhu Li,*, [†] Benli Wang, [‡] Jian Liu, [†] Zhiyuan Li, [‡] Lei Jiang, [†] and Yanlin Song*, [†]

[†]Beijing National Laboratory for Molecular Sciences (BNLMS),

Key Laboratory of Organic Solids, Laboratory of New Materials,

Institute of Chemistry, Chinese Academy of Sciences, Beijing, 100190, China

[‡]Laboratory of Optical Physics, Institute of Physics, Chinese Academy of Sciences, Beijing 100190, China

E-mail: ylsong@iccas.ac.cn; mingzhu@iccas.ac.cn

This journal is © The Royal Society of Chemistry 2012

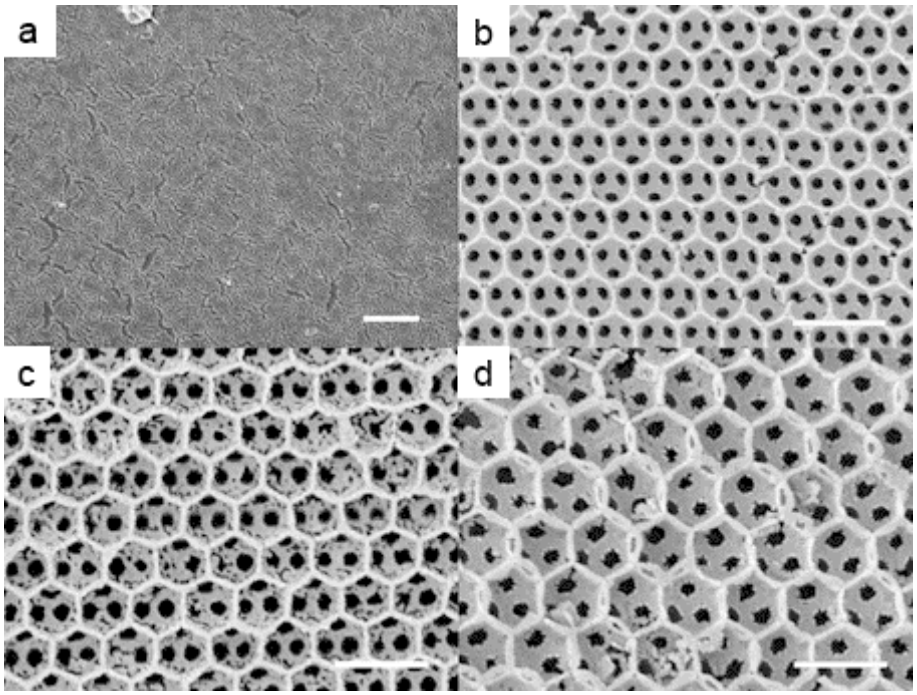

Fig. S1. The SEM images of the inverse opal (IO) and GNPs coated glass slide (Au-GS). The SEM images of (a) Au-GS (the control sample), (b) IO_{229}, (c) IO_{279} and (d) IO_{320} (scale bar: 500 nm). The GNPs coated glass slide is used as the control sample. The inverse opals with different lattice constants were fabricated from different templates. The opal templates have the sphere diameters of 300 nm, 330 nm and 380 nm. The lattice constants of inverse opals are all smaller than the sphere diameters of templates because of the TiO_2 skeleton shrinkage in the calcination process. The lattice constants of inverse opals for the IO_{229}, IO_{279} and IO_{320} are 229 nm, 279 nm and 320 nm, respectively.

This journal is © The Royal Society of Chemistry 2012

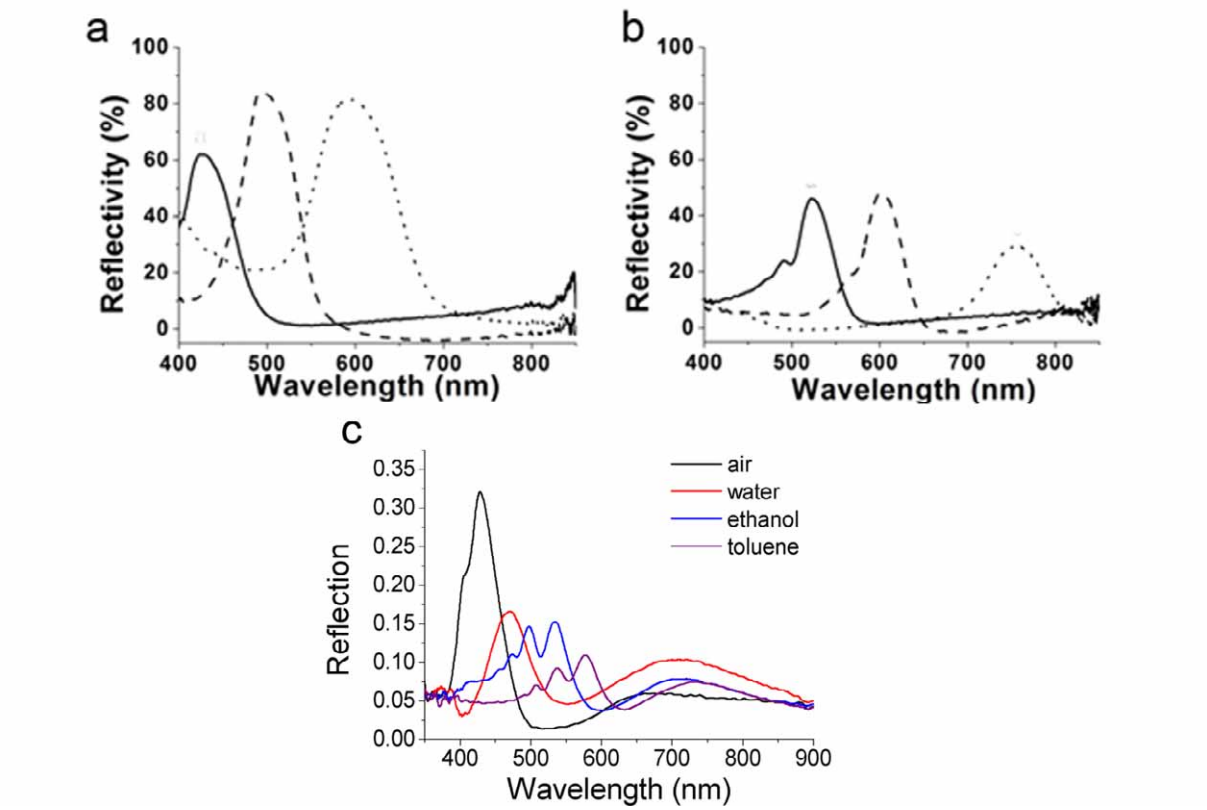

Fig. S2. The stop bands of the inverse opals. The reflection spectra of IO_{229} (solid line), IO_{279} (dash line) and IO_{320} (dot line) (a) in air and (b) in water. (c) The reflection spectra of Au-IO_{188} in the air, water, ethanol and toluene, respectively. The stop bands for all these inverse opal samples are illuminated from these reflection peaks. It is shown that all the reflection peaks red shift, and their intensities relatively reduced in the solutions. Following the Bragg's law,

$$\lambda = 1.633 \times d \times \sqrt{f_{pores} \times n_{pores}^{2} + f_{framework} \times n_{pores}^{2}}$$

When the n_{pores} changes from the n_{air} as 1.0 to the n_{water} as 1.33, the $n_{ethanol}$ as 1.36, and the $n_{toluene}$ as 1.49, the wavelengths (λ) of the reflection peaks will increase. At the same time, the decreases of the refractive index (RI) contrast between the two dielectric materials ($n_{framework}$ = n_{TiO2} =2.46, n_{pores} changing from 1.0 to 1.33, 1.36 and 1.49) reduce the depth of the stop bands. Therefore, choosing the high RI material for the frameworke of the inverse opal is important to keep the depth of stop band in the in-solution detection. In this experiment, the TiO_2 with a high RI as 2.46 was chosen as the framework material of the inverse opal. The deep stop bands are acquired in water. Au-IO_{188} in the air, water, ethanol and toluene have the stop bands red shift and reduced due to the above reason. The mutiple peaks is observed for Au-IO_{188} in ethanol and toluene when the stop band shift to the wavelength range of the LSPR (λ = 500 ~ 600 nm). This result shows the combination of the photonic and plasmonic properties for manipulating the incident light.

This journal is © The Royal Society of Chemistry 2012

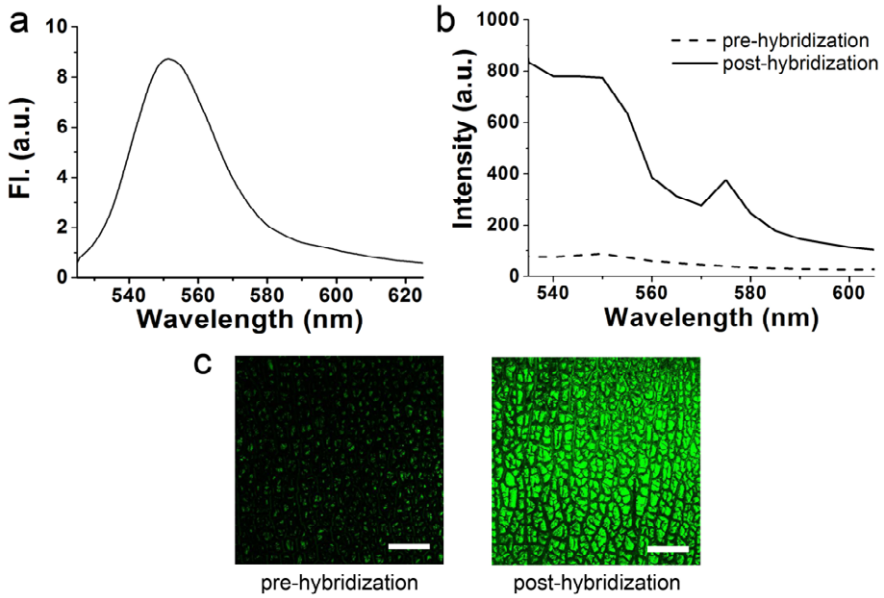

Fig. S3. The fluorescence spectra. (a) The fluorescence spectrum of the HEX labeled molecular beacon (MB) solution (0.3 μM) in Tris-HCl buffer soluiton (pH 7.2, 0.1 M). The emission maximum of the fluroscent labeled MB is at the wavelength of 551.4 nm (λ_{ex} = 515 nm). (b) The fluorescence spectra and (c) the confocal fluorescent micrographs (scale bar: 50 μm) of the Au-IO before (pre-hybridization) and after (post-hybridization) the SARS detection. These fluorescence spectra and micrographs are collected by the confocal laser scanning microscope (FV1000, Olympus) with 5 nm per step, excited by a 515 nm laser. The intensities of the fluorescence peaks at 550 nm indicate the value of detection signals. It is shown that the fluoresence is greatly enhanced after hybridization.

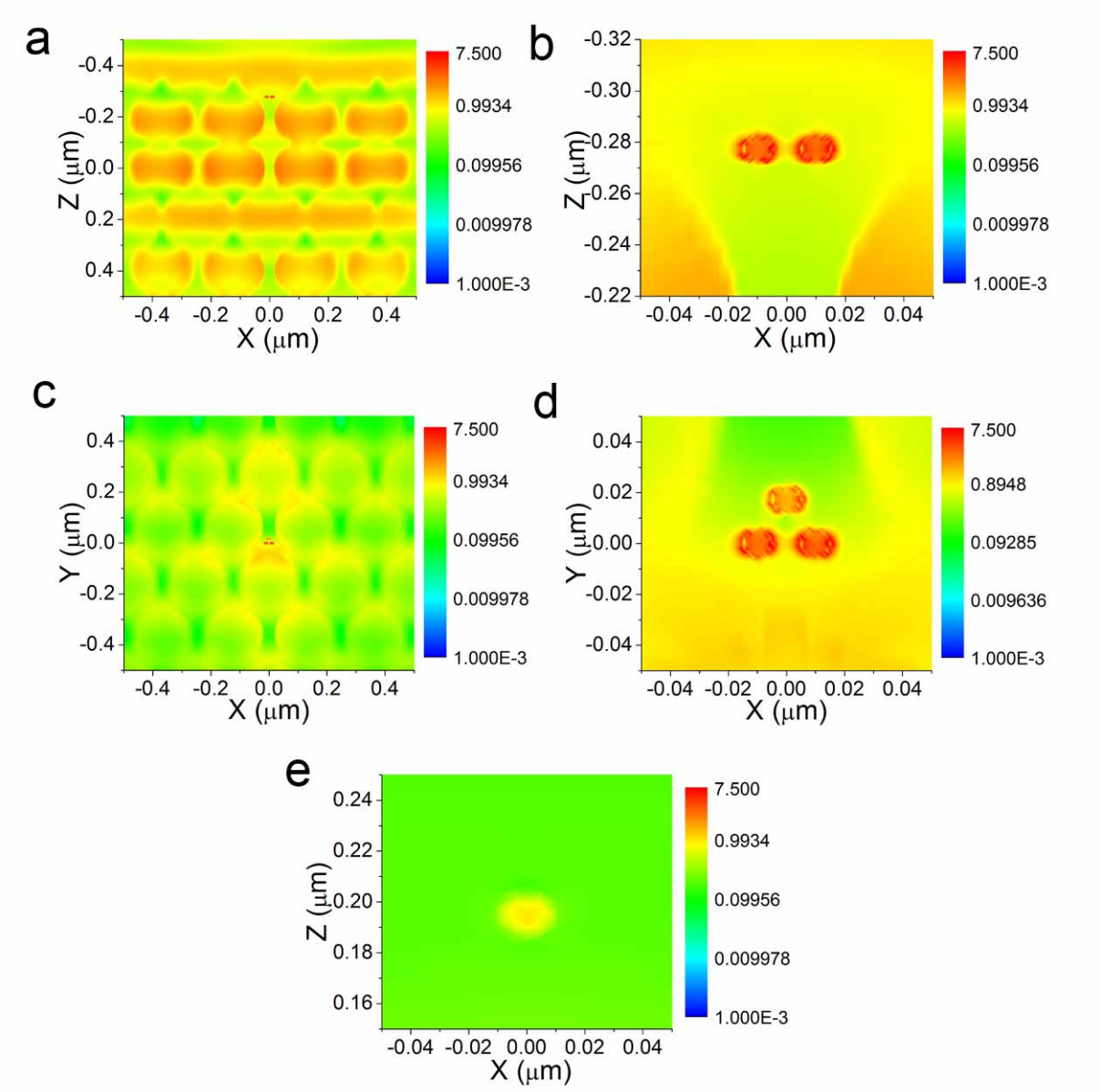

Fig. S4. Theoretical calculations on the optical field patterns. The cross sectional patterns of the simulated electric field for the Au-IO on (a, b) x-z plane and (c, d) x-y plane. (e) The situation of single gold nanoparticle on glass slide (Au-GS) is also simulated for comparing the intensity of electric field. The finite-difference time-domain (FDTD) method was employed in the simulation. The model of the simulation is a 6-layers TiO_2 inverse opal with three gold nanoparticles in its pore in the surface layer. The period of inverse opal is set to 245 nm, and the refractive index (RI) of TiO_2 is set to 2.46. The three GNPs with the diameters of 10 nm are placed in the bottom center of a surface pore. The inter-particle distances of the GNPs are set to 10 nm. The surrounding is the water with RI as 1.33. It is shown that the inverse opal can localize the incident light (λ = 515 nm) in the pores. The localized intense field around the GNPs can further excite the LSPR of the GNPs. The intensity maximum of the Au-IO is *ca.* 4.7 times as large as that of the Au-GS.

This journal is © The Royal Society of Chemistry 2012

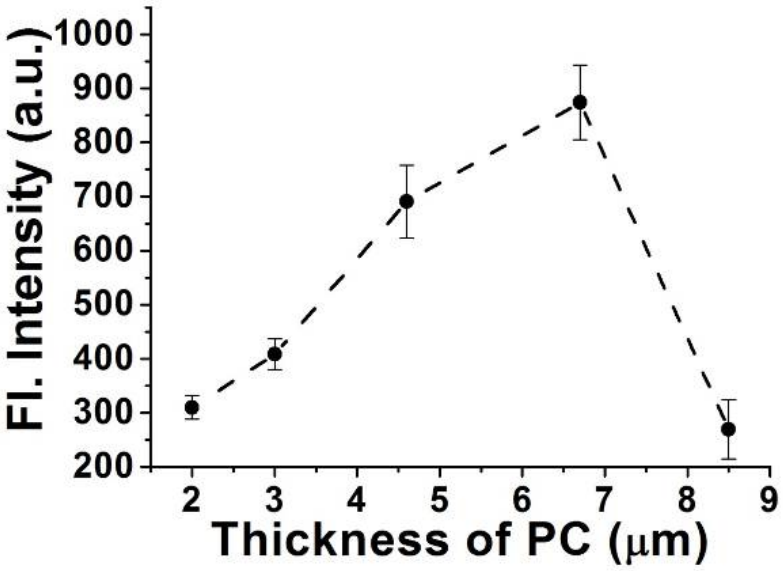

Fig. S5. The fluorescence intensities with defferent inverse opal thicknesses. The thickness is important for the optical properties of PC. The thickness of inverse is controlled through changing the latex concentration of template spheres.When the PC thickness is less than 6.8 μm, the thicker the PC, the more intense the fluorescent signals. Increasing the number of repetitive units on Z axis will enhance the ability of inverse opal to localize the incident field. However, when the thickness of inverse opal is 8.5 μm, the disorders and cracks greatly increase, resulting in decrease of the fluorescent signal. Thus, the optimzed thickness of inverse opal is determined to 6.8 μm.

This journal is © The Royal Society of Chemistry 2012

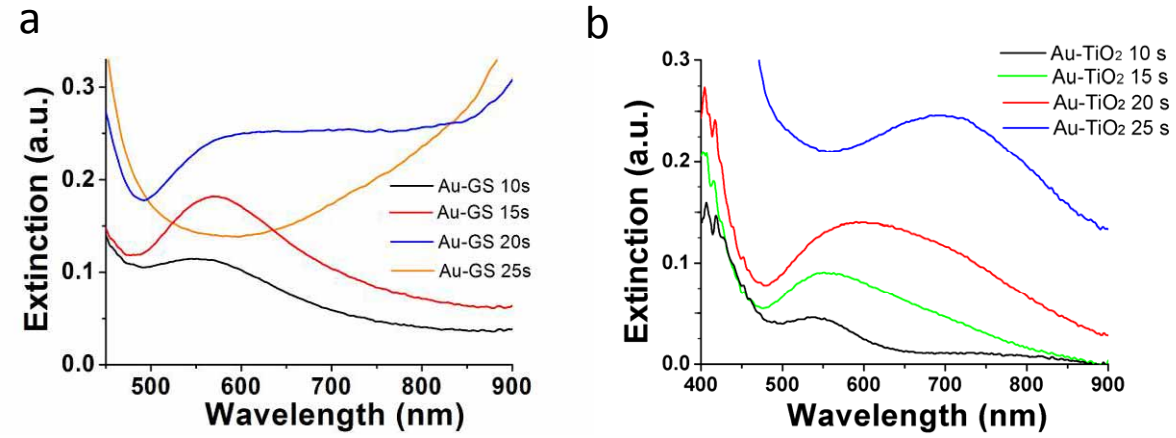

Fig. S6. The extinction spectra of (a) Au-GS and (b) Au-TiO_2 samples with the different sputtering time of the GNPs. The change of the LSPR peaks depending on the sputtering time of GNPs is clearly shown. When the sputtering time is 10 s, the LSPR peak appears at the wavelength of 551 nm. With the sputtering time of 15 s, the LSPR peak becomes sharper. When sputtering the GNPs for 20 s, the LSPR peak still enhances, but the base line at long wavelength side ascends. This phenomenon indicates that the GNPs begin to aggregate to some larger clusters and generates some long-wavelength SPR extinction. Finally, the LSPR peak completely disappears when the sputtering time is 25 s. In this situation, the Au-GS has the aggregated GNPs. The GNPs on the glass slide from dispersion to aggregation are with the sputtering time from 10 s to 25 s. In the text, the GNPs on inverse opal from dispersion to aggregation are with the sputtering time from 30 s to 180 s. The GNPs on glass slide aggregated much faster than that on the inverse opal because the glass slide has much less surface area for dispersion of GNPs. The extinction spectra of GNPs coated TiO_2 films (Au-TiO_2) with the sputtering time from 10 s to 25s were also collected. The TiO_2 film was fabricated by dip coating glass slide in the TiO_2 precursor sol and calcination. The extinction peak wavelength of Au-TiO_2 red shift from 537 nm to 698 nm in company with increasing the sputtering time from 10 s to 25 s. This phenomenon can be also attributed to aggragation of GNPs.

This journal is © The Royal Society of Chemistry 2012

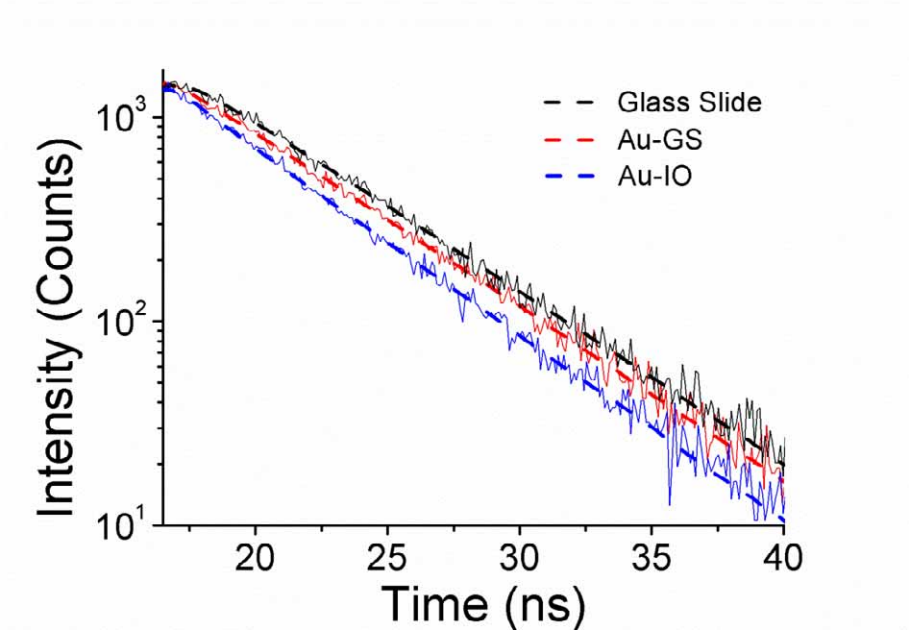

Fig. S7. The Fluorescence decay curves from fluorescence DNA solution (Probe MB1) on glass slide, Au-GS and Au-IO. The dash lines are fits of the exponential function to the data. Emission spectra were obtained using a FLS920 time-resolved spectrofluorometer (Edinburgh Analytical Instruments). The curves are recorded at λ= 550 nm and T = 298 K with 515 nm excitation source. The samples are with the fluorescence DNA solution (10 μl, 50 μM) and coated by cover glasses. The most fluorescent molecules dissolved in the solution between the sample and cover glass, and a few fluorescent molecules adsorbed on the sample surface. The signal of surface adsorbed fluorsecent molecules corresponds to the hierachical optical antenna experiment result. The two kinds environments of the fluorescent molecules make the fluorescence decay curves fit the double exponential function:

$$I = \alpha_1 \exp (- t / \tau_1) + \alpha_2 \exp (- t / \tau_2)$$

where the τ_1 and τ_2 are the fluorescent liftime with amplitude α_1 and α_2, and $\alpha_1 + \alpha_2 = 1$. The lifetime of the fluorescent DNA on glass slide is T_0 = 4.7 ns, calculated from the single exponential function ($I_0 = \alpha \exp (- t / \tau_0)$). For the Au-GS, the lifetime are τ_1 = 4.72 ns (α_1 = 0.94) and τ_2 = 2.6 ns (α_2 = 0.06). The τ_1, the same lifetime to the τ_0, is ascribed to the most flurescent DNA in the solution. The τ_2, the shorter lifetime than the τ_0, is ascribed to a few flurescent DNA adsorbed on the gold nanoparticles. The plasmonic particle can reduce the fluorescence lifetime of the fluorophore near its surface, which is a proof of metal enhanced fluorescence (MEF) effect.[1] For the Au-IO, the decay time are τ_1' = 4.3 ns (α_1' = 0.90) and τ_2' = 1.0 ns (α_2' = 0.10). The τ_1', the similar decay time to the τ_0, is ascribed to the most flurescent DNA in the solution. The τ_2', the shorter decay time than the τ_0 and τ_2, is ascribed to a few flurescent DNA adsorbed on the gold nanopartles modified inverse opal (Au-IO). The lifetime of the τ_2' is shorter than the τ_2, which proves that flurescent DNA adsorbed on the Au-IO further enhanced by the photonic structure besides the MEF effect from the gold nanoparticles. Furthermore, the τ_1' is smaller than the τ_0 and τ_1, which proves that the inverse opal PC has the ability of reduction the lifetime and enhance the fluorescence to the fluorophores not on its surface but in the pores. The inverse opal PC enhance the fluorescence due to its strong coherent scattering and the increased distribution width of the decay rate.[2] It has been proved that large inhibitions and enhancements of the spontaneous emission can be achieved with properly positioned and oriented efficient dipolar light sources inside 3D photonic crystals. Therefore, it is proved that the Au-IO is a more effective optical antenna the the bare GNPs with the hierachical enhancement mechanism.

This journal is © The Royal Society of Chemistry 2012

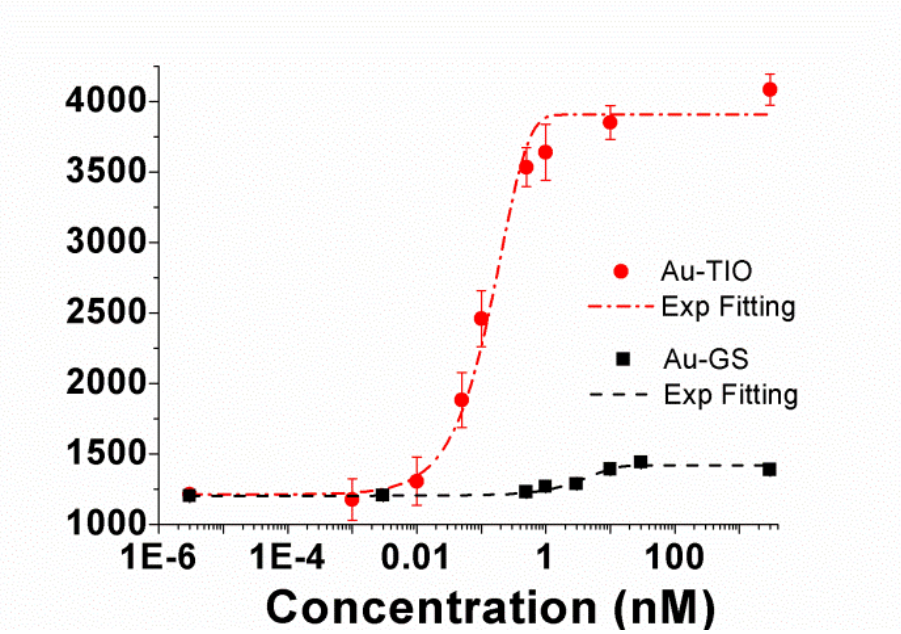

Fig. S8. The detection results of SARS on the Au-IO and Au-GS. The Au-GS is used as the control sample for comparing the enhancement of detection limit. The amount of GNPs on the control is controlled same with that on the Au-IO by utilizing the same sputtering currents (20 mA) and sputtering time (60 s). The detection signals are greatly enhanced on the Au-IO substrate compared with that on the control sample. The detection limit on the control sample is *ca.* 0.310 nM, and that of the Au-IO is *ca.* 0.030 nM. There is over one order of magnitude improvement of the detection limit on the Au-IO comparing with the Au-GS.

1. Lakowicz and J., *Anal. Biochem.*, 2002, **301**, 261-277.
2. I. S. Nikolaev, P. Lodahl, A. F. van Driel, A. F. Koenderink and W. L. Vos, *Physical Review B*, 2007, **75**, 115302.